22nd International Conference
ENGINEERING MECHANICS 2016
Svratka, Czech Republic, 9 – 12 May 2016

EXPERIMENTAL ANALYSIS OF TORSION VIBRATION OF HARD RUBBERS UNDER LARGE DEFORMATIONS

P. Šulc[*], L. Pešek, V. Bula, J. Cibulka, J. Košina

Abstract: *The paper deals with a stress analysis of hard rubber under large torsion deformations. This study was motivated by effort to enhance the theoretical background for experimental evaluation of material behaviour of hard rubbers on our test rig. First the Mooney Rivlin model (MRM) for shear case of loading was developed and then MRM constants were attained by fitting of the MRM to the experimental torsion-deformation curve. Then the tuned MRM cylindrical model was tested under torsion loading for evaluation of stress state. Besides the radial distribution of shear stress and strain the attention was paid to evaluation of axial stresses. It could help to assess the influence of the tension stresses on the tangential deformations of the test sample during large torsion.*

Keywords: hard rubber, torsion vibration, large deformation, hyperelasticity, parameter identification

1. Introduction

For rubber materials unlike conventional structural materials under dynamic loading, a nonlinear time-varying behavior occurs due to the size of straining, creep, temperature and aging (Pešek, 2008). Tests of rubbers with higher hardness Sh 50-80 (Nashif, 1985) were performed in the laboratories of IT AS CR in recent years. The dynamic tests of hard rubbers require usually a costly long-term operation of heavy hydraulic machines. Therefore we have started to look for realization of the tests in laboratory conditions with the lighter laboratory technique. Currently we have been developing a torsional dynamic test rig for torsional straining of hard rubber samples with a circular cross-section (Šulc, 2014). The reason for torsion straining was that hard rubber materials are softer in torsion than in pressure and therefore it is easier to achieve larger strains. Furthermore at this straining the shape changes are smaller in comparison with pressure loading when so-called barreling effect arises due to incompressibility of the material.

The torsional test rig should serve to dynamic material tests of hard synthetic rubbers for determination of the thermo-viscous-elastic material characteristics under small as well as finite strains, different amplitudes, frequencies and temperatures. This paper deals with the stress analysis of cylindrical samples at larger shear strains (up 10%), which leads to analysis of a nonlinear dependence of shear stress on shear strain and initiation of tensile component along the axis of the sample at larger torsion deformations.

Hence, the aim was to evaluate this stress component to assess its influence on the overall straining of the test sample. Therefore a numerical finite element model (FEM) of a rubber cylinder under the torsional stress considering hyperelasticity and finite strains was created in ANSYS. The five-parametric Mooney-Rivlin model (MRM) was considered. To calculate the constants of the MRM model, analytical relation between shear stress and shear strain were derived. The relation served for identification of the MRM constants on a base of tuning of the constant to achieve an optimal agreement between analytical and experimental stress-strain curves. Finally, the results and analysis of the numerical calculations of the three-parametric MRM model by the FEM are presented.

2. Hyperelastic model of rubber for shear straining

The strain energy of five-parametric MRM model can be expressed as

[*] Ing. Petr Šulc, PhD., Ing. Luděk Pešek, CSc., Ing. Vítězslav Bula, Jan Cibulka, Ing. Jan Košina : Institute of Thermomechanics of the CAS, v. v. i., Dolejškova 1402/5; 182 00, Prague; CZ, sulc@it.cas.cz

$$W = C_{10}(I_1 - 3) + C_{01}(I_2 - 3) + C_{20}(I_1 - 3)^2 + C_{11}(I_1 - 3)(I_2 - 3) + C_{02}(I_2 - 3)^2 \qquad (1)$$

where W is a strain energy and I_1, I_2 are invariants of the Green strain tensor.

Torsion straining of the cylindrical surface is analogous to the straining in a simple shear. Deformation gradient F for the simple shear strain is determined by

$$\mathbf{F} = \begin{pmatrix} 1 & \gamma & 0 \\ 0 & 1 & 0 \\ 0 & 0 & 1 \end{pmatrix} = \mathbf{R} \cdot \mathbf{U} \qquad (2)$$

where γ is the shear strain of a segment of the cylinder. Strain gradient **F** is decomposed by polar decomposition to a rotational tensor **R** and a strain tensor **U** (right "stretching" tensor). Then for Green's strain tensor $\mathbf{C} = \mathbf{F}^T\mathbf{F}$ and strain tensor **U** holds

$$\mathbf{C} = \mathbf{F}^T\mathbf{F} = (\mathbf{RU})^T\mathbf{RU} = \mathbf{U}^T\mathbf{R}^T\mathbf{RU} = \mathbf{U}^T\mathbf{U} = \mathbf{U}^2. \qquad (3)$$

To determine the principal strains in the “main” directions under the simple shear consideration, first we calculate the Green's strain tensor **C**

$$\mathbf{C} = \mathbf{F}^T\mathbf{F} = \begin{pmatrix} 1 & \gamma & 0 \\ \gamma & 1+\gamma^2 & 0 \\ 0 & 0 & 1 \end{pmatrix}. \qquad (4)$$

Then eigenvalues of the Green strain tensor are equal to principal strains of the strain tensor **U**

$$\lambda_1 = U_1 = \sqrt{C_1} = \frac{\sqrt{4+\gamma^2}+\gamma}{2},\ \lambda_2 = U_2 = \sqrt{C_2} = \frac{\sqrt{4+\gamma^2}-\gamma}{2},\ \lambda_3 = U_3 = \sqrt{C_3} = 1. \qquad (5)$$

To get MRM constants, we determine the invariants of Green strain tensor by principal strains

$$I_1 = \lambda_1^2 + \lambda_2^2 + \lambda_3^2, \quad I_2 = \lambda_1^2\lambda_2^2 + \lambda_2^2\lambda_3^2 + \lambda_1^2\lambda_3^2, \quad I_3 = \lambda_1^2\lambda_2^2\lambda_3^2. \qquad (6)$$

At simple shear deformation there is no volume change. It holds when the third invariant of the Green strain tensor equals to 1 and $\lambda_3 = 1$, too. So, we can express a relation between the remaining two principal strains $\lambda_1 = 1/\lambda_2$. Substituting the strain tensor eigenvalues (principal strains) of (5) into the invariants (6) we get these relations

$$I_1 = 3 + \frac{\gamma^2}{2}, \quad I_2 = 3 + \frac{\gamma^2}{2}, \quad I_3 = 1. \qquad (7)$$

Constitutive relation for Cauchy stress expressed in principal strains is

$$\sigma_a = -p + \lambda_a \frac{\partial W}{\partial \lambda_a}, \qquad a = 1,2,3 \qquad (8)$$

where p is the Lagrange multiplier also called hydrostatic pressure. The constant *p* is determined incompressible materials from the condition $\sigma_3 = 0$ (Holzapfel, 2000).

If we come from the expressions of the Cauchy principal stress (8) for the simple shear straining of cylindrical surface, after derivation of the strain energy over invariants I_1 and I_2 of the Green strain tensor and after substituting $\lambda = \lambda_1$, $\lambda_2 = \frac{1}{\lambda}$. We can express it in the form

$$\begin{aligned}\sigma_1 &= -p + 2\left(\lambda^2 - \frac{1}{\lambda^2}\right)\left(\frac{\partial W}{\partial I_1} + \frac{\partial W}{\partial I_2}\right)\\ \sigma_2 &= -p + 2\left(1 - \frac{1}{\lambda^2}\right)\left(\frac{\partial W}{\partial I_1} + \lambda^2\frac{\partial W}{\partial I_2}\right)\end{aligned}. \tag{9}$$

After substitutions and derivations of (9) the Cauchy principal stresses for five-parametric MRM model were arranged (Šulc, 2016) as

$$\begin{aligned}\sigma_1 &= -p + 2C_{10}\left(\lambda^2 - \frac{1}{\lambda^2}\right) + 4C_{20}(I_2 - 3) + 2C_{11}\left(\lambda^2 - \frac{1}{\lambda^2}\right)(I_1 - 3) +\\ &+ 2C_{01}\left(\lambda^2 - \frac{1}{\lambda^2}\right) + 4C_{02}\left(\lambda^2 - \frac{1}{\lambda^2}\right)(I_1 - 3)\end{aligned} \tag{10}$$

$$\begin{aligned}\sigma_2 &= -p + 2C_{10}\left(1 - \frac{1}{\lambda^2}\right) + 4C_{20}(I_2 - 3) + 2C_{11}\left(1 - \frac{1}{\lambda^2}\right)(I_1 - 3)(1 + \lambda^2) +\\ &+ 2C_{01}\left(1 - \frac{1}{\lambda^2}\right)(I_1 - 3) + 4C_{02}\lambda^2\left(1 - \frac{1}{\lambda^2}\right)(I_1 - 3)\end{aligned}.$$

The final relation for the maximal shear stress from principal stresses σ_1, σ_2 by use of (10) is

$$\tau_{\max} = \frac{1}{2}(\sigma_1 - \sigma_2). \tag{11}$$

The constants of the MRM are evaluated from the experimental shear stress-strain curve using the least square method (LSM) (Šulc, 2016).

3. Numerical results of torsion straining of rubber cylinder under larger strains

Experimental shear stress-strain curve of selected hard rubbers for the MRM constant tuning was obtained by our torsion test rig for a temperature -20°C. The test specimen was of cylindrical shape glued at both heads to steel consoles pins mounting in the collets. By usage of the consoles the test sample is not deformed in the vicinity of the heads due to clamping. The dimensions of the test sample of rubber were: ∅D = 0.05 m, length L = 0.036 m and weight 0.0763 kg. The material was isoprene butadiene rubber (IB) of hardness Sh60 and shear modulus of 11 MPa for a shear strain below 1%, temperature -20°C and frequency 20Hz of torsional loading. Experimental shear stress-strain curve (maximum value of strain is about 8%) is shown in Figure 1. Tuned constants of the three and five-parametric MRM models based on LSM method result in:

a) C_{10} = -0.0224e^9, C_{11} = -0.8023e^9, C_{01} = -0.0075e^9, C_{20} = -2.4963e^9, C_{02} = 1.3316e^9

b) $C_{10} = -1.5610e^7$, $C_{11} = -1.1975e^7$, C_{01} = 0.5211e^7 .

The relations (1-10) result analogically for three-parametric MRM model where $C_{20} = C_{02} = 0$ (Šulc, 2016). For comparison, the shear stress-strain curves of three- and five-parametric models of MRM together with experimental counterpart are plotted on Figure 2.

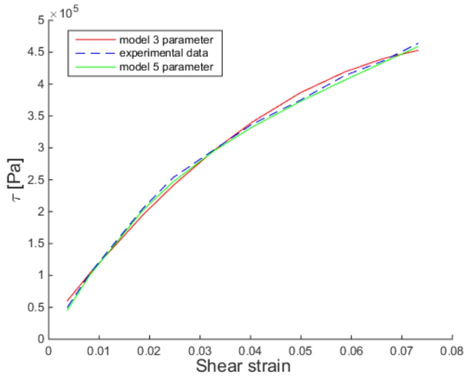

Fig. 1: Comparison of experimental shear stress-strain curve with counterparts of three- and five-parametric MRM models

It is obvious that the five-parametric MRM model fits better to the experimental data. For numerical simulations we come from the cylinder of diameter ∅D = 0.05 m and length l = 0.02. The cylinder was fixed in all nodes of the basis head and was loaded over a rigid plate connected to the upper head of the cylinder by the torque moment M_k=22.5Nm. Two material models, a) elastic model (G = 33MPa), b) three-parametric model MRM with the experimentally tuned constants, were used for the stress and deformation analysis. Linear model corresponds to the analytical solution to a size of shear stresses, tangential displacements and their space distribution. MRM model behaves almost linearly in this range of deformations and gives slightly smaller tangential deformation with respect to the linear model. This difference are caused by different methods of deformation solution (linear versus non-linear) including different representation of the stress-strain curve (Fig.1). The distribution of tension stress σ_{zz} over the surface of the specimen calculated for the non-linear MRM model (case b) is shown in Fig.2. It can be seen that the axial stresses are non-uniformly distributed in the volume of the specimen and their maximal stresses concentrate along the axial axis of the specimen and attenuate with the radial distance from the axis.

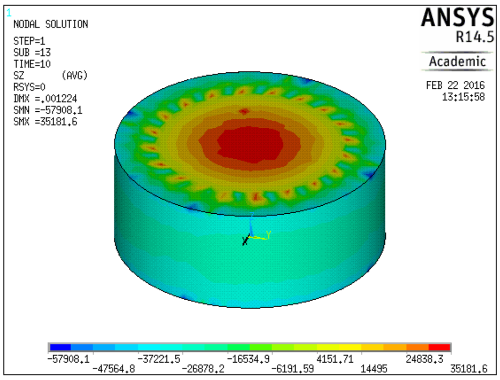

Fig. 2: The contour map of tension stress σ_{zz} distribution over the surface of the sample

By comparing maximal values of the shear and axial stresses for this study case, it is obvious that a size of axial stresses achieve very small values (about 25 times smaller) related to a size of shear stresses at shear deformations at cca 20%.

4. Conclusions

The aim of this paper was to evaluate the influence of the axial stresses arising at cylindrical samples of hard rubbers under large torsional deformations. Therefore the analytical relation for the simple shear stress-strain dependence of the five-parametric MRM model was derived. Both the constants of five-parametric model and analogically the three-parametric MRM model were calculated from the experimental stress-strain curve that we ascertained for the isopren-butadien rubber Sh60. The combined stress distributions of rubber cylinder under the torsional loading and larger strains were calculated by FE method using three-parametric MRM model. The results showed that a non-linearity is very weak for assumed shear strains (up to about 20%). As to the axial stresses it was found that they concentrate mainly around the cylinder specimen axis and reach relatively low maximal values with respect to the maximal values of shear stresses. It can be, therefore, assumed that the side effect of axial stresses does not significantly influences an accuracy of standard evaluation of rubber constants based on the linear theory of elasticity.

However, these theoretical findings are to be validated by the experiment. The torsion scale with a possibility to evaluate the axial tensile force has been developed in our lab and the first experimental results will be shown at the oral presentation at the conference.

Acknowledgement
This research work has been elaborated under financial support for conceptual development of research institutions RVO: 61388998 in the Institute of Thermomechanics, v.v.i., Prague.

References

Holzapfel A. G.(2000) Nonlinear Solid Mechanics, John Wiley&Sons.

Nashif, A. D., Johnes D. I. G., Henderson J. P. (1985): Vibration Damping, John Wiley&Sons.

Pešek, L., Půst, L., Balda, M., Vaněk, F., Svoboda, J., Procházka, P., Marvalová, B.(2008) Investigation of dynamics and reliability of rubber segments for resilent wheel, Procs. of ISMA 2008, KU Leuven, pp. 2887-2902.

Šulc P., Pešek L., Bula V., Cibulka J.,Košina J.(2015) Amplitude-temperature analysis of hard rubber by torsional vibration. Applied Mechanics and Materials - Archive of EM2015.

Šulc P., Pešek L., Bula V., Cibulka J., Košina J.(2016) Přídavná osová napjatost pryžového válce při torzním namáhání a velkých deformacích. Dymamesi 2016. Praha : Institute of Thermomechanics AS CR, v.v.i, s. 57-65.